International Journal of Steel Structures
https://doi.org/10.1007/s13296-024-00891-y

Online ISSN 2093-6311
Print ISSN 1598-2351

Monotonic Pushover analysis of Externally Reinforced Welded I-column to foundation Connection

Saraswati Setia[1] · C. V. R. Murthy[2] · V. K. Sehgal[1] · Subhash Magapu[1]

Received: 25 September 2023 / Accepted: 23 August 2024
© Korean Society of Steel Construction 2024

Abstract
This study presents an improved understanding of the stress distribution in the joint region of weak-axis connections in steel MRFs, and based on this understanding, connection configurations have been proposed for the column-to-foundation connections Columns in MRFs are subjected to lateral forces along their strong and weak axes. To ensure ductile response, analysis, and requisite provisions of column foundation connections along the strong axis have been dealt with in detail. In this study, preliminary inelastic finite element analyses are conducted to study the flow of forces near the weak axis column-to-foundation connection. Theoretical axial load *P* in the column that produces the worst *V-M (shear-moment)* loading is identified. Based on these loads a cover plated and ribbed configuration is proposed for the weak- axis column-base (WACB) connection. Nonlinear finite element analyses are performed under monotonic, and FEMA recommended multi-cycle loadings using ABAQUS software to evaluate the performance of the proposed connection configurations and the associated design procedures. The performance of the new weak-axis connections (WACs) is compared with that of the existing connections in terms of von Mises stress, shear stress, normal stress, load deformation response, energy dissipated, and cumulative plastic strain excursion. It was observed that WACB connections in steel MRFs need to be reinforced to keep the stress in CJP welds connecting the column to the base plate below the yield stress even at the lateral drift levels much lower than those expected of about 4–6% lateral drifts. The proposed configuration results in increased moment of inertia of the column about the weak axis and hence enhances the seismic response.

Keywords Weak Axis · Connections · Seismic design · Steel · Stress concentration

1 Introduction

In moment-resisting frames, the load essentially flows from the beams through the beam-to-column connections to the columns, and finally through the column–to-foundation connections to the foundation. Thus, column-to-foundation connections in steel moment-resisting frames (MRFs) are required to transfer the column loads, from all possible load combinations (including those due to seismic shaking) to the underlying foundation. Under intense seismic forces, MRFs experience the creation of plastic hinges at the bases of columns, occurring in both sway and story mechanisms before reaching the point of ultimate load or collapse. The emergence of these mechanisms places significant inelastic demands on the connections between columns and foundations. To enable the formation of plastic hinges in the columns, the column-to-foundation connections must possess sufficient strength to withstand the most crucial combination of axial load, maximum potential overstrength bending moment, and related shear force. The ductile behavior of the column-to-foundation connection is critical to the overall response of the building under strong seismic condition. Much of the attention on performance of steel MRFs in past earthquakes was focused on performance of beam-column joints; little attention was paid to column-bases. Further, since the number of collapses of steel MRFs were few, damages to column-bases were either overlooked, or attributed to poor foundation concrete strength, poor workmanship, and geotechnical foundation problems. During the 27 March 1964 Prince William Sound, Alaska earthquake, the six-story Cordova building, having a steel frame as its primary

✉ Saraswati Setia
ssetia@nitkkr.ac.in

[1] Department of Civil Engineering, NIT Kurukshetra, Kurukshetra, Haryana, India

[2] Department of Civil Engineering, IIT Madras, Chennai, Tamil Nadu, India

Published online: 31 August 2024

lateral load resisting system suffered column-base failures. These failures were attributed to poor quality welds, spalling of footing concrete, etc., (FEMA-355E, 2000). Evidence of column base damage in steel moment resisting frames, documented after the 1964 Anchorage earthquake, resurfaced in the 1994 Northridge and 1995 Kobe earthquakes. Even though steel buildings collapsed during the 19 September 1985 Mexico City earthquake, it was primarily attributed to column buckling failures, but not column-base failures. Following the 17 January 1994 Northridge earthquake, extensive damage to column-base plate connections was reported. The Northridge earthquake highlighted the vulnerability of column-bases, though primarily attention was focused on fractures at welded beam-to-column connections in MRFs. The usual column-base connection comprises columns welded to a base plate, which is then anchored onto a concrete pedestal using four anchor bolts. Failures in this connection type were observed to include (a) fractures occurring in the base plate, extending through its entire thickness and width, (b) the pullout of anchor bolts, and (c) horizontal cracks along the welds that connect the column flanges to the base plate (Krawinkler et al., 1996). The thick base plate was suspected of acting as a heat sink and cooling faster than the column flanges during the welding process of the column to the base plate. This resulted in residual tensile stresses in the base plate, which contributed to the initiation of fractures in this area. Anchor bolt pull-out, accompanied by concrete pedestal cracks, was also observed at several locations. The concrete pedestal crushing in one case indicated a significant vertical impact of the base plate against the concrete. This impact could have been exacerbated by the earthquake's unusually large vertical component of ground shaking. (Bertero et al., 1994). Significant drifts in the upper story of the buildings were attributed to base-plate fracture and consequent base plate rotation (Fig. 1) (Latour et al., Jun. 2014).

Fig. 1 Fracture of 100 mm thick base plate created by overturning moments in braced bays following 1994 Northridge earthquake: These fractures appeared to start at the fillet welds connecting the columns to the base plates (Bertero et al. 1994)

2 Behaviour of Column-Base Plate Connection

Each structural component of the base plate connection, namely, the concrete pedestal, anchor bolts, base plate and the column end reinforcing elements, play a critical role in the overall functioning of the column-base connection. Besides, welds are also important in smooth and safe transfer of loads from the column to the base connection. Further, in general, depending on the type of loading on the column-foundation assembly, three primary modes of failure are possible, namely failure in (a) shear resistance, (b) moment resistance, and (c) tensile resistance (Salmon et al., 1957). Besides, another possible failure mode is in compression resistance. These are manifested through failures of the individual components of the connection scheme. The functions and the possible failure modes of the components in base plate connection are discussed in the following sub-sections.

2.1 Concrete Pedestal

A concrete pedestal primarily transfers column loads safely to the soil, supporting the base plate and securing anchor bolts. Concrete exhibits nonlinear compression behaviour but linear tension behaviour with much lower strength. Under typical conditions, the pedestal fails due to concrete compression crushing beneath the base plate. In an experiment by DeWolf et.al., 19 square base plate concrete cube specimens were axially loaded until failure. (DeWolf, 1978). Tests revealed load increase after initial cracking, followed by load reduction with strain; average cracking load to ultimate load ratio was approximately 0.8. Failed specimens formed inverted cones/pyramids under the plate, causing concrete cube splitting. Pedestal depth significantly impacted ultimate load in axial loading. In a second test program, 3 benchmark specimens were studied, subjected to axial loads only, along with moments on steel columns over concrete pedestals. (DeWolf & Sarisley, 1980). Concrete failure was abrupt due to differing confinement levels in two tests. In one test, direct machine placement added confinement, while the other eliminated it by fixing column assemblies. Regardless, concrete under the base plate formed pyramids upon failure. Axially loaded specimens had truncated pyramids, while moment-loaded ones had complete ones. Thambiratnam and Paramasivam conducted study with 12 specimens, low-moment ones failed due to concrete crushing at the base plate's bearing area. Concrete cracks started at the top surface and moved down. In high-moment cases, failure resulted from base plate or anchor bolt yielding. The primary pedestal failure mode is compression-induced

concrete crushing, with research focusing on design bearing stress. The anchor bolt-pedestal interaction is vital in column-foundation connections, especially under high moments and shear, involving concrete tensile failures in anchor bolts. (Thambiratnam & Paramasivam, 1986) (Fig 2).

2.2 Base Plate

The column resists axial, shear, and moment forces, transferred through the full cross-section when both flanges and the web are active. The base plate's main task is evenly distributing the column load onto the concrete pedestal. Experiments on column-base plates under axial compression and moments found minimal concrete bearing stress at the plate's edges but a peak under the column's position. (Cannon, 1992; DeWolf, 1978; DeWolf & Sarisley, 1980; Thambiratnam & Paramasivam, 1986). The uneven bearing stress under the base plate results from the plate's flexibility, leading to bending. Consequently, localized bearing stress between the base plate and the concrete pedestal can reach up to 6 times the concrete's compressive strength ($6f_c$) without compromising the column-to-foundation connection's ultimate strength. (Cook et al., 1989). Increased lateral loads shift the pressure bulb in the concrete foundation from the column center towards the base plate's edges in the load direction. The bearing stress on the foundation depends on the base plate's flexural stiffness. Thicker base plates can evenly distribute stress, while less rigid ones may concentrate stress under the column's flanges and web, with only some areas effectively carrying compression. As the ratio of base plate thickness to the distance from its edge to the column face decreases, the base plate's flexibility becomes more influential in stress distribution. (Aviram & Stojadinovic, 2006). Thinner base plates reduce concrete contact, concentrating stress at column flanges, while thicker plates act rigidly, causing edge stress. Stress becomes irregular near concrete's capacity. Thicker plates enhance load capacity but excessive thickness may not improve lateral capacity, causing plate lift-off and concrete crushing, especially with the thickest plates. Thin plates under axial loads and moments develop plastic hinges, leading to a gradual load drop. Design methods often use an equivalent rectangular stress distribution pattern, akin to the Whitney compression block in reinforced concrete LRFD design. (ACI 318–02 & ACI 318R–02, 2002). The column's bending moment is balanced by a tension–compression force couple, with the lever arm equal to the distance between the resultant of concrete bearing stresses on the compression side of the base plate and the centerline of the anchor bolts on the tension side. To find the maximum bending demand in the base plate, we compare bending effects: double curvature due to tensile forces in the column flange and anchor bolts on the tension side versus cantilever bending from bearing stress on the compression side. The greater of these effects determines the maximum bending demand on the base plate. (Drake & Elkin, 1999). In the transition area between tension and compression, the base plate encounters high shear stresses. Three mechanisms provide shear resistance and horizontal equilibrium for the column base connection:(a) Friction between the concrete surface and the steel base plate, which functions as the effective

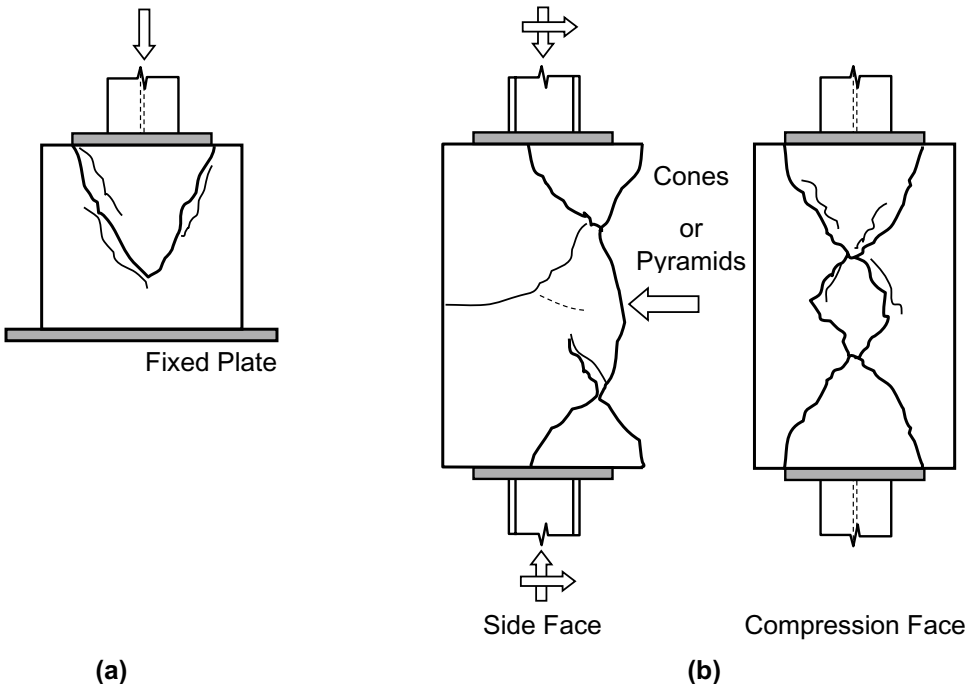

Fig. 2 *Cone failure of concrete*: Complete cones below base plate **a** under pure compressive loading with column attachment on one side only, and **b** under combined compressive and shear loading with column attachment on either sides (You & Lee, 2020)

bearing area for compressive loads. (b) Bending and shear in the anchor bolts. (c) Shear lugs positioned under the base plate (or on the side of an embedded base plate) that bear against adjacent concrete or grout. When subjected to lateral loads, axial compression, or anchor bolt preload due to external moments, the base plate initially transfers shear forces through frictional resistance between the base plate and the concrete pedestal. (Rabbat & Russell, 1985). For concrete-steel interface specimens, bond strength ranged from 0.17 to 0.61 MPa, while grout-steel interface specimens exhibited negligible bond strength. However, the average coefficient of static friction was 0.65 for steel and concrete and 0.68 for steel and grout (Cook & Klingner, 1992).

2.3 Anchor Bolts

The primary role of anchor bolts is to resist external moments through tension–compression couple. A common mode of failure of base plate connections with axial compressive loads and moments is yielding of base plate followed by tensile yielding of anchor bolts in the tension region. But, under tension, pull-out cone failure of anchor bolts can occur owing to inadequate bolt diameter, small bolt embedment, small bolt-to-foundation edge distance and insufficient concrete load bearing capacity (Peier, 1983; Ueda et al., 1990; Zhao et al., 2022). The bond between anchor bolts and concrete is critical. Bolt-concrete bond slip can happen with inadequate embedment or smooth bolt surfaces. To enhance mechanical anchorage, hooked anchor bolts are used but tend to fail through straightening and pull-out of concrete. In contrast, anchor bolts with embedded nuts offer better anchorage, providing a more effective way to resist forces and reduce the risk of pull-out failures. (Cui et al., 2021; Marsh & Brudette, 1985; Shipp & Haninger, 1983). Anchor bolts primarily resist external shear forces through friction between the base plates and the concrete pedestal. In the proposed behavioral model, anchors in the compression zone initially handle shear forces. Only when their shear strength is exceeded does the remaining shear transfer to anchors in the tension zone. The shear strength of tension zone anchors is constrained by their combined tension and shear capacity. However, this study did not account for frictional resistance between the base plate and concrete pedestal, which can significantly affect behavior and load transfer. Moreover, bearing failure in the concrete around anchor bolts, particularly under substantial shear forces and inadequate bearing capacity, must be considered. Analyzing and designing column base plate connections should account for these factors to ensure safety and stability under diverse loads. (Hawkins et al., 1980; Lynch & Burdette, 1991; You & Lee, 2020).

3 Present study

Preliminary inelastic finite element analyses are conducted for unreinforced WACB connections of 2 m long column stubs to study the flow of forces in the joint. Column base loading is complex because of simultaneous action of *P*, *V* and *M*. Infinite combinations of *P*-*V*-*M* exist in building frame WACB connections. There is no guidance on the type of loading to be considered in the study of WACB regions. In this study, two load conditions are used to study flow of forces in the WACB region, namely (i) pure shear displacement loading till 4% lateral drift, and (ii) combined axial compressive load and shear displacement loading till 4% lateral drift; the axial compression is incrementally increased to P_y at 4% lateral drift. The first case corresponds to lightly loaded column subjected to lateral drift, and the second to, the leeward column under seismic shaking where the axial load increases with lateral displacement. The axial load and lateral displacement are applied at the top of the joint-sub-assemblages.

Along the weak axis, each column flange is subjected to tensile as well as compressive forces simultaneously. A sudden change in the flow of forces from the vertical plane to a horizontal plane saddled with an abrupt change of geometry results in a complex pattern of flow of forces at the column foundation joint. The unreinforced weak axis column-base connection analyses result in the following observations (Fig. 3): (i) Even under pure gravity loading, there is concentration of stresses at the reentrant corners where the forces traverse from the vertical to the horizontal plane; Fig. 3a shows the behavior at the end of application of compressive load equal to 50% of the yield axial load P_y; (ii) further, when the lateral force comes into play, the yielding of the CJP welds that connect the column to the base plate occurs at as low as 0.25% drift levels; and (iii) at 1% drift levels, the compression side of the column flange and the base plate underneath shows high distress. These observations clearly indicate the necessity of reinforcing the joint region so as to provide a logical load path, which allows a smooth transition for the flow of forces from the column to the foundation and also shifts the plastic hinge formation away from brittle welds to the column section.

Based on the observations on flow of forces at the weak axis column-to-base joint, it is concluded that the plastic hinge initiates at a point above the end of connection reinforcement. This point of initiation of plastic hinge is identified as the *truss point*, which is useful in developing a truss model for estimating the forces on the column-to-foundation connections. The distance of this truss point from the end of the column-to-foundation connection reinforcement region, is called the *truss length* l_t. This is taken as half the column depth, *i.e.*,

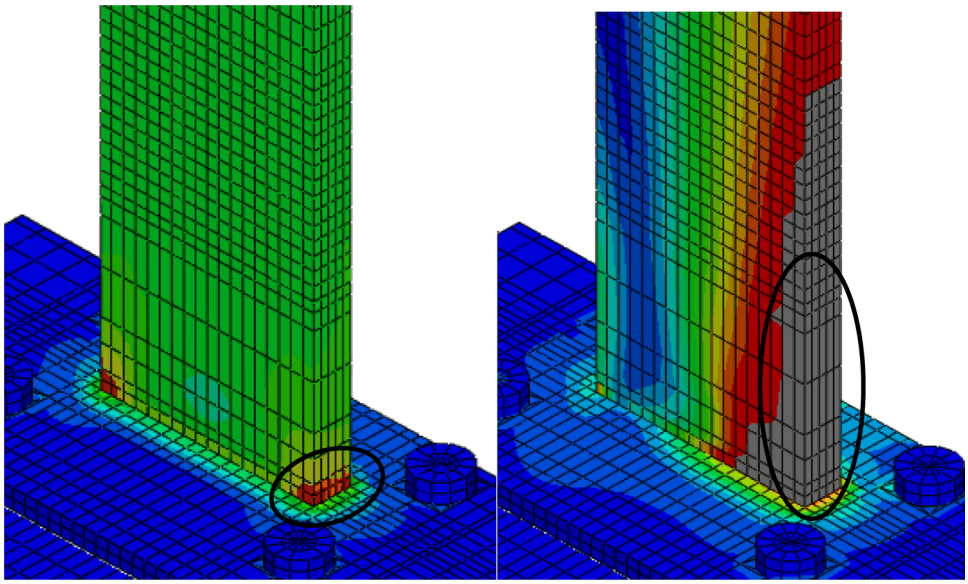

(a) (b)

Fig. 3 *Behavior of unreinforced weak-axis column- base connection subjected to shear axial loading*: **a** Stress contours at the end of gravity loading indicate stress concentration at the reentrant corners **b** Excessive column flange and connecting weld yielding at 1% drift levels.

$l_t = \frac{d_c}{2}$;

where d_c is the depth of the column. Using this, two different strut-and-tie models are used to represent the flow of forces near the connection region – one to represent the action of V alone, and the other the continued action of P and M. The twin-truss model along with the design forces are shown in Fig. 4.

This study addresses this gap through preliminary inelastic finite element analyses, focusing on the force flow in the weak-axis column-to-foundation connection. The theoretical axial load (P) in the column is determined, considering the most critical combination of shear (V) and bending moment (M) loading. Based on these loads, a proposed design involves a cover-plated and ribbed configuration for the weak-axis column-base (WACB) connection. To validate this design concept, nonlinear finite element pushover analyses are conducted on column-base sub-assemblages designed using this approach. These sub-assemblages undergo testing with four different loading scenarios, encompassing the expected range of forces typical for interior and exterior column-base connections in steel MRFs during severe seismic loads.

3.1 Nonlinear Finite Element Analysis

In this study, numerical investigations are done through monotonic displacement-controlled nonlinear finite element analysis using ABAQUS (HKS, 2005). The study involves analyzing weak-axis column-base joint-sub-assemblages. Each typical joint-sub-assemblage consists of a column with a length equal to half the column height at the ground floor level (using centerline dimensions. To take advantage of symmetry, only a symmetric half of the sub-assemblages is modeled since the loadings and sub-assemblages are symmetric about a vertical plane (z = 0) passing through the column centroid. The materials used in the models include ASTM 572 Grade 50 steel for columns and connection elements, with a yield strength (Fy) of 345 MPa. The connecting weld material, E70 electrode, has a yield strength of 345 MPa and an ultimate tensile strength of 480 MPa at 20% elongation. The anchor bolts used are made of ASTM A36 grade steel (Fy = 250 MPa), and both materials have the same initial elastic modulus of elasticity (E) of 200 GPa and Poisson's ratio of 0.3. The concrete used in the foundations is of grade 30 MPa in terms of characteristic cylinder compressive strength. Both material and geometric nonlinearity are considered in the analyses. The material nonlinearity of the steel is considered using a classical isotropic plasticity model based on the von Mises yield criterion and associated plastic flow. The column-base joint-sub-assemblages and CJP (Complete Joint Penetration) welds are modeled using 8-node linear solid brick elements. 6-node linear wedge elements, with three translational degrees of freedom at each node. The bottom nodes of the concrete pedestal are fully restrained in the models. Conventional analysis assuming the base plate to be rigidly connected to the concrete pedestal, i.e., *fixed*-base condition overestimates the response both in terms of strength and stiffness in most cases of the sub-assemblages. This indicates that full fixity is difficult to achieve in column bases with anchor-bolted base

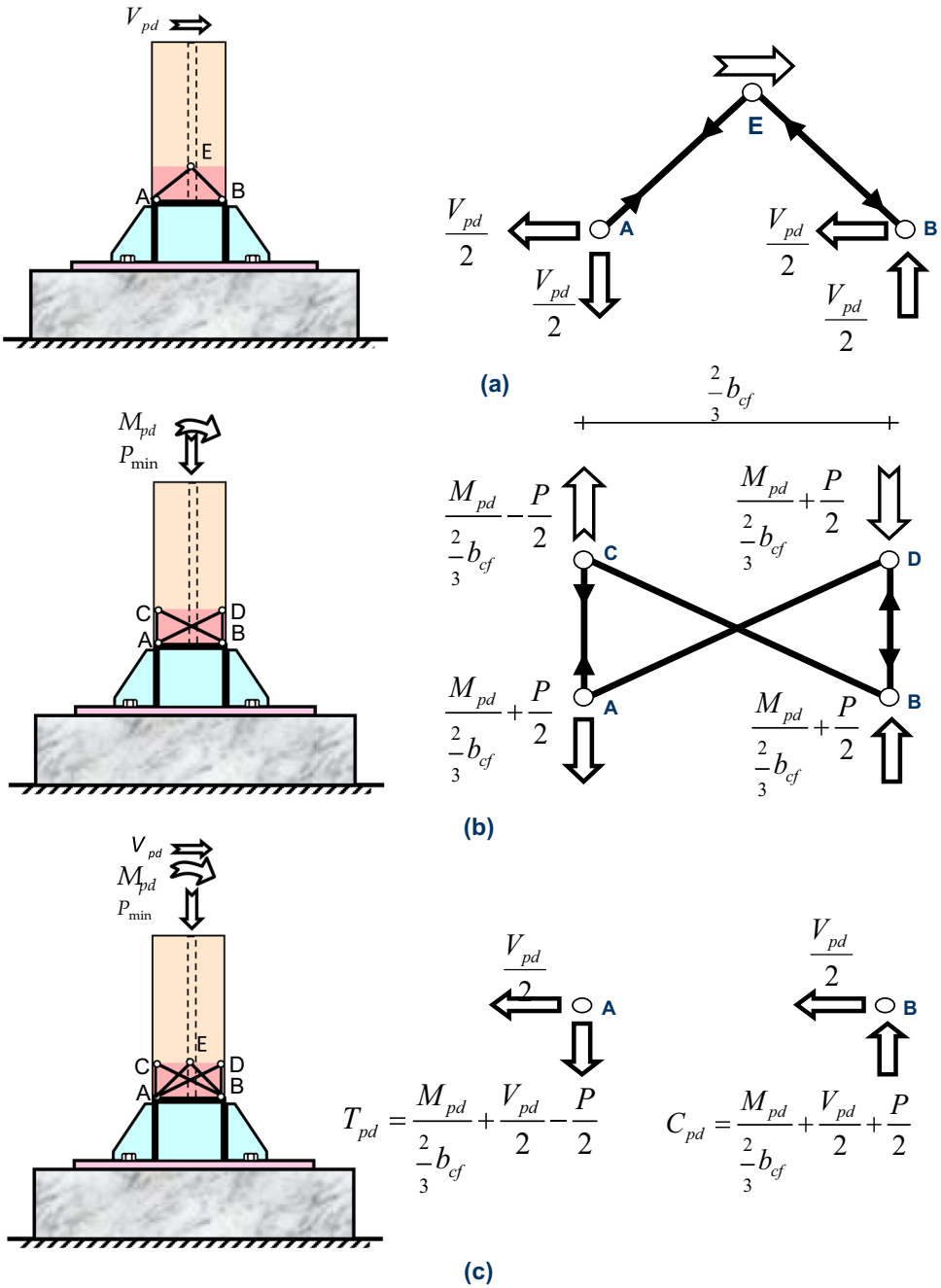

Fig. 4 *Twin Truss Model*: Connection design forces based on flow of forces based on **a** *V* truss, **b** *P-M* truss, and **c** Net connection design forces

plate connections. Moreover, to get a rational estimate of the moment rotation characteristics of such column bases, actual base conditions must be simulated in the finite element analysis (Goswami, 2008; Grilli et al., 2017). Hence, the base plate over the concrete pedestal is not physically connected to the concrete pedestal; *surface interaction* is used. This surface interaction allows for sliding and uplift of the base plate, thus simulating actual behavior of the connection. The normal behavior is modeled using hard contact interaction that allows separation after contact (if required, as in case of subsequent uplift). The tangential behavior between the solid elements is modeled with friction having a friction coefficient of 0.4. The hard contact normal interaction option available in the ABAQUS software is used to model the anchor head-base plate interaction and the anchor bolt shank-base plate interaction. The anchor bolt nodes are connected to the corresponding nodes of the pedestal simulating infinite anchorage because the anchor bolts are designed to preclude any failure (including pullout failure) (Figs. 5 and 6).

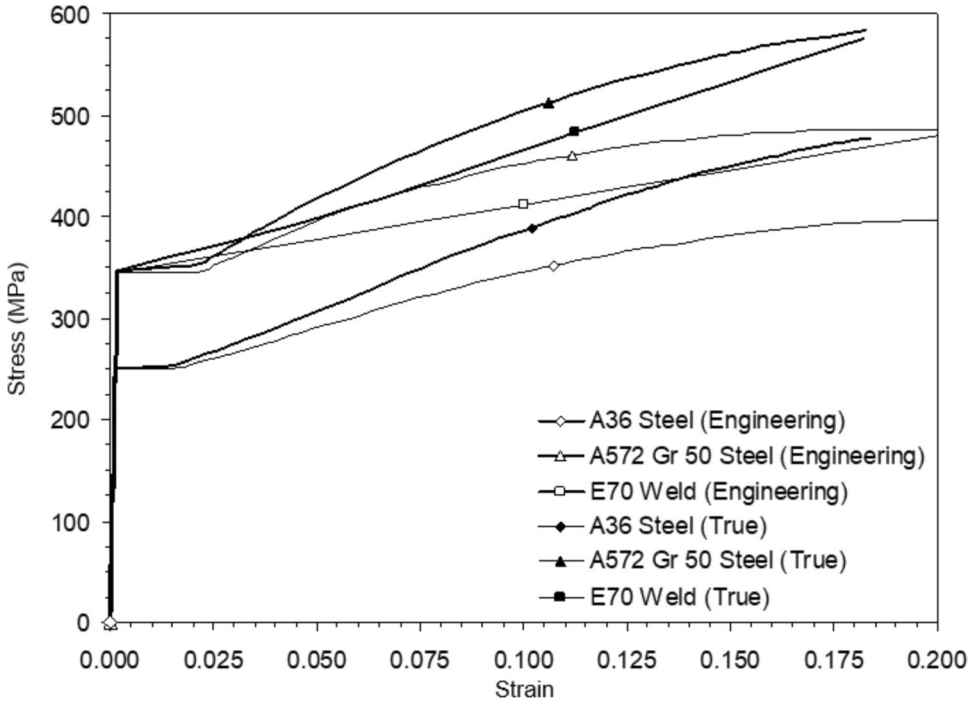

Fig. 5 *Material constitutive laws*: Engineering and true stress–strain curves of the different materials used in analyses. All three materials have the same Young's modulus (200 GPa) and Poisson's ratio (0.3)

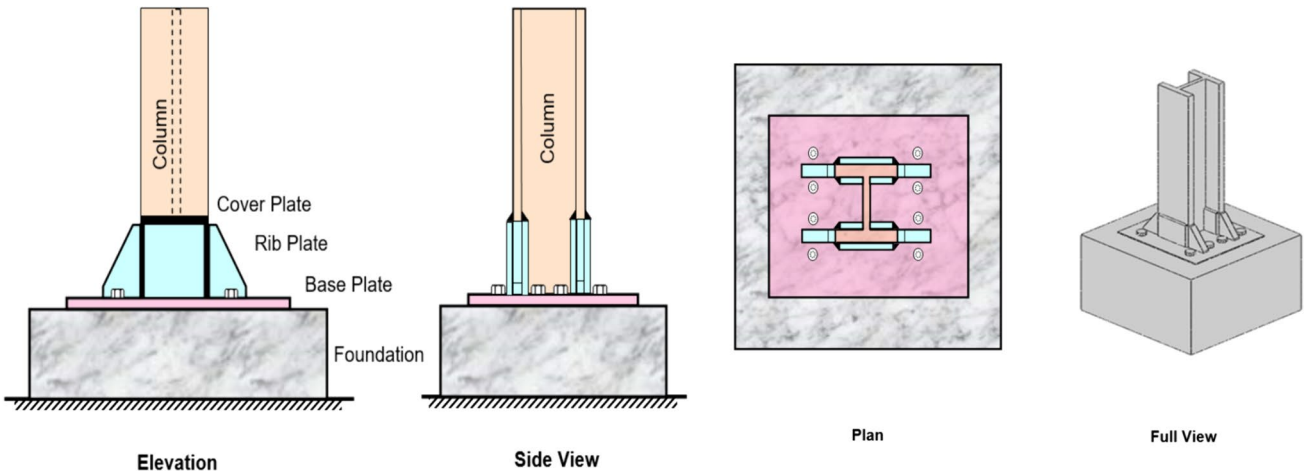

Fig. 6 *Reinforced weak-axis column-to-foundation connection scheme*: Cover plated rib plated connection over anchor-bolted base plate to ensure smooth flow of forces in the joint

3.2 Analysis of Proposed Connection Configuration

Connections (cover plates, vertical rib plates and connecting welds) of 10 WACB joint-sub-assemblages are designed using the developed design procedure for weak axis column-to-foundation connections assuming an axial compressive load of 40% of the yield capacity of the column P_y acting on the column along with the corresponding moment and shear. Base plate, concrete pedestal, and anchor bolts are designed by standard procedures. Nonlinear monotonic displacement-controlled pushover analyses are performed of these sub-assemblages up to 4% lateral drift Δ to assess their overall post-elastic load-deformation response and to validate the proposed configuration and design procedure. The overall geometry, loading conditions and boundary conditions of the sub-assemblages are shown in Fig. 3. Figure 4 shows a typical finite element discretization (column W14 × 398). Table 1 lists the column sizes, dimensions of the connection elements (including headed anchor bolts) and concrete pedestal of the sub-assemblages. The table also lists the design loads considered in the study. The columns sizes are chosen so as to represent a possible range of column

Table 1 Design loads and dimensions of weak axis column-to-foundation connection components:

#	Column Section	Design loads on column base			Cover Plate			Rib Plate			Base Plate			Pedestal			Anchor bolt
		P (kN)	M (kNm)	V (kN)	lcp	bcp	tcp	hrp	brp	trp	lbp	bbp	tbp	lped	bped	dped	Ø
1	W14×730	19,141	7510	12,600	382	385	35	382	221	125	1200	1200	24	2000	2000	1000	51
2	W14×500	13,110	5400	8680	405	382	25	405	234	89	1200	1000	31	1750	1750	1000	51
3	W14×398	10,405	3720	6820	350	380	21	350	202	73	1200	1000	39	1725	1725	1000	51
4	W30×391	10,240	2930	6750	305	356	20	305	176	70	1000	1200	27	1725	1725	1000	32
5	W27×368	9619	2620	6340	322	338	18	322	186	63	1000	1200	22	1725	1725	1000	29
6	W36×300	7866	2300	5270	305	395	15	305	176	51	1000	1250	21	1750	1750	1000	26
7	W12×252	6583	1830	4470	282	298	16	282	163	57	850	750	12	1200	1200	1000	39
8	W24×207	5410	1310	3580	288	306	12	288	166	40	900	1000	18	1750	1750	1000	23
9	W21×147	3837	886	2530	278	298	10	278	161	29	850	850	14	1500	1500	1000	20
10	W16×100	2650	525	1720	230	244	10	230	133	25	750	750	12	1200	1200	1000	20

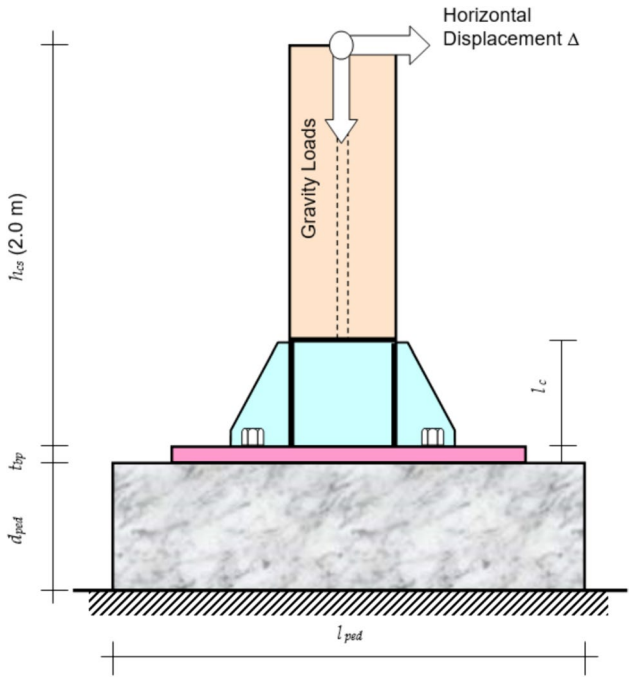

Fig. 7 *Geometry, loading conditions and boundary conditions of WACB joint-sub-assemblage*: The base plate is anchor-bolted to the concrete foundation which is assumed to be fixed at the base

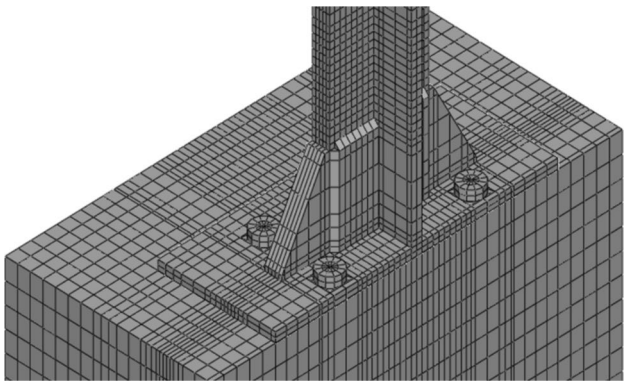

Fig. 8 *Finite element model of column-base sub-assemblage*: 8-node and 6-node linear solid elements are used with special inter-surface interactions between (i) pedestal and base plate, (ii) anchor bolts and base plate, and (iii) column flange and cover plate.

sizes that could be used in low-rise to medium-rise MRFs (Figs. 7 and 8).

3.3 3.3 Loadings Considered

The column-to-foundation sub-assemblages are subjected to the four types of pushover loadings, each in two steps. In the first step, the axial load (P_y) is applied and pushover load (case a,b) and in the second step, axial load and monotonic axial load (P^*) plus pushover load is applied (case c,d).

4 (a) ($0.2P_y$) plus Pushover of (80 mm)

A compressive load P equal to $0.2P_y$ and a monotonic horizontal displacement Δ of 80mm (4 %) at the free end of the column in increments.

5 (b) ($0.5P_y$) plus Pushover of (80 mm)

A compressive load P equal to $0.5P_y$ and a monotonic horizontal displacement Δ of 80 mm (4%) at the free.

end of the column in increments.

6 (c) ($0.5P_y$) plus Pushover of ($0.5P_y$ and 80 mm)

A compressive load P equal to $0.5P_y$ and additional monotonic compressive load P^* equal to $0.5P_y$ and monotonic horizontal displacement Δ of 80 mm (4 %) at the free end of the column simultaneously in increments.

7 (d) ($0.5P_y$) plus Pushover of ($-0.4P_y$ and 80 mm)

A compressive load P equal to $0.5P_y$ on the column and additional monotonic tensile load P^* equal to $0.4P_y$ and monotonic horizontal displacement Δ of 80 mm (4%) at the free end of the column simultaneously in increments.

7.1 3.4 Weak-Axis Column-Base Connection Response

The truss length of the ten column-to-foundation sub-assemblages under (i) pure shear loading, and (ii) axial compressive load and bending moment are determined. These are tabulated in Table 2. The values are shown at two lateral drift levels; 0.33% lateral drift signifies elastic condition, while 1.00% signifies a state when inelasticity is expected to have been initiated but not to a great degree. Under pure shear loading in the elastic state, i.e., at 0.33% drift, the average truss length to depth ratio is 0.41, but with increased drifts instead of inelasticity spanning into the column flange, it shifts towards the connection region, which is indicated by the value of 0.36. Under axial compressive load coupled with bending moment, the truss length is still lower. This means that the assumed truss length of $0.5d_c$ is an upper bound estimate, except in the elastic state in the mid-web under pure shear loading. At 0.33%, 1% and till the anchor bolts have not yielded, the truss point follows the $0.5d_c$ assumption. But, at higher drifts, the anchor bolts have yielded so no inelasticity is mobilized in the column, and hence there is a drop in the truss point values. All forces are transferred to the anchor bolts. Anchor bolts lose their stiffness at higher drift values.

Table 2 *Truss length in weak-axis column-to-foundation connections*: A design value of $0.5d_c$ is proposed as truss length for WACB connection design.

Column	Truss Length to Column Depth Ratio (l/d_c) under different loading conditions			
	Pure Shear At Mid-web		Axial Compression and shear in compression side of flange	
	Drift		Drift	
	0.33%	1.00%	0.33%	1.00%
W14×730	0.47	0.40	0.53	0.29
W14×500	0.51	0.51	0.57	0.31
W14×398	0.51	0.40	0.51	0.34
W30×391	0.32	0.32	0.32	0.16
W27×368	0.36	0.27	0.38	0.29
W36×300	0.27	0.27	0.32	0.17
W12×252	0.48	0.33	0.50	0.37
W24×207	0.41	0.32	0.45	0.34
W21×147	0.38	0.38	0.38	0.22
W16×100	0.36	0.36	0.36	0.23
Average	**0.41**	**0.36**	**0.43**	**0.27**

Figure 9 shows the observed truss lengths l_t in web and compression flange at 0.33% and 1.00% lateral drifts for the ten sub-assemblages studied. In all the cases, the observed truss length to column depth ratio is lower than the assumed values. Broadly, it can be concluded that the efficiency of the configuration will be determined by the strength and stiffness of the anchor bolts at higher drift levels than on itself.

Inelastic finite element analyses of the 10 column-to-foundation sub-assemblages are performed for the four load Cases (a) to (d) simulating actual base conditions with provisions of base plate sliding and uplift. From the 40 analyses results (Fig. 10), the following important observations are made:

1) For the sub-assemblages under load cases (a), (b), and (d), nonlinear response begins at about $0.55H_{pc}$, while sub-assemblages under load Case (c), nonlinear response begin at about $0.30H_{pc}$. This difference in the starting of nonlinear response is due to the difference of the initial gravity load; $0.20P_y$ in loading Cases (a) and $0.50P_y$ in loading Cases (b), (c) and (d). The relatively large initial gravity load of $0.50P_y$ in loading Cases (b), (c), and (d) prevents early overturning of the column over the foundation; this increases the reserve elastic capacity of the column-foundation sub assemblage.
2) Tension yielding of anchor bolts and base plate uplift are major causes of early nonlinear response of the sub assemblages, particularly in windward columns (*i.e.*, load Cases (a) and (d)).
3) For load Case (c), the lateral load-drift curves drop rapidly after attaining the peak value. In this case, an additional gravity load of $0.50P_y$ is applied along with the lateral drift in addition to the initial gravity load of $0.50P_y$. Thus, for higher steps of pushover analysis, the axial load on the columns approaches the axial capacity P_y of the columns; this is reflected as the dropping part of the lateral load-drift curve.
4) Tables 3 and 4 show the level of inelasticity mobilized in the joint at 1% and 4% lateral drift levels. The maxi-

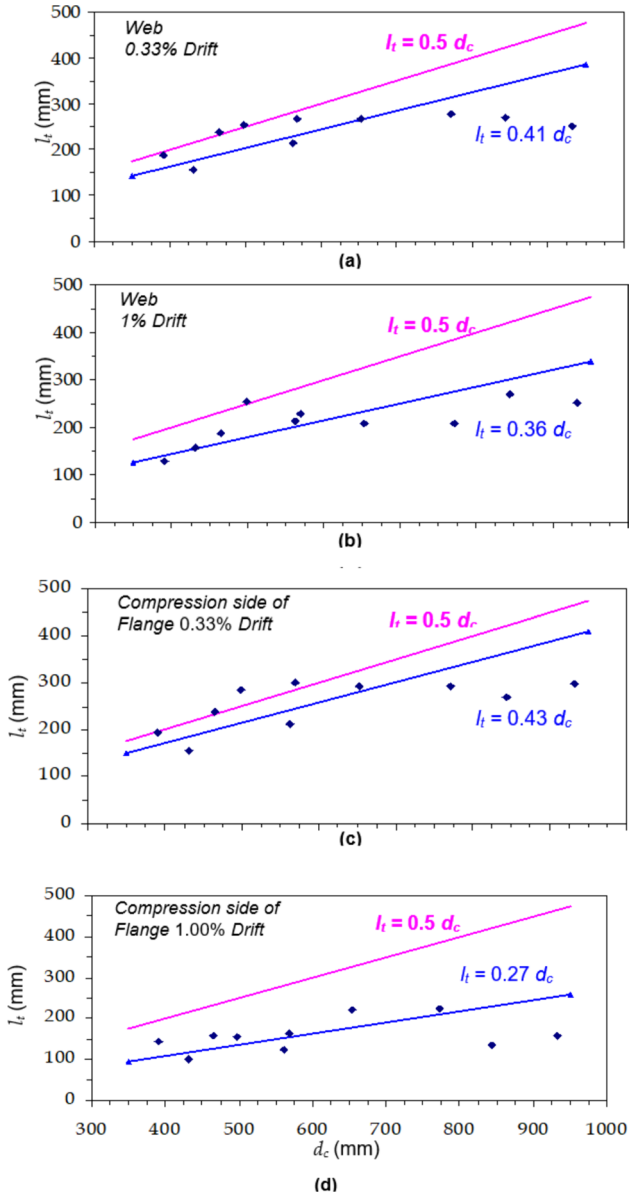

Fig. 9 *Truss length from the 10 weak-axis column-to-foundation subassemblages*: Linear best fit results for **a** 0.33% drift at web, **b** 1.00% drift at web, **c** 0.33% drift at compression side of flange, and **d** 1.00% drift at compression side of flange. The figure also shows the proposed truss length $l_t = 0.5d_c$ for weak-axis column-to-foundation connection design

mum average lateral load resisted at 1% lateral drift is about the same in all the four cases varying from 57 to 67%. But the trend is not followed at higher drift levels. The maximum average lateral load resisted is only 85% in load Case (b) at 4% lateral drift. In load Cases (a) and (d), 88% and 75% of the lateral load corresponding to plastic hinge formation in the column is resisted. At higher drift levels the failure of the anchor bolts restricts the spread of inelasticity into the column flange. In load Case (c), there is a sharp decrease in the lateral load resistance of the column due to high initial axial gravity load.

5) The design of connection plates and welds are critical in heavily loaded leeward columns, while the design of anchor bolts is critical in all other columns; base plate uplift induces additional bending, along with tension, in anchor bolts.
6) In heavily loaded columns, the proposed cover-plated rib-plated connection configuration effectively reinforces the column near the column-to-foundation connection and pushes inelasticity away from the joint into the column section (Fig. 11). Also, the CJP welds connecting the column to the base plates are not stressed beyond the design strength.

M_{pc} or H_{pc} has not been attained in any case. The reason is assumed partial fixity; the present connection configuration does not provide full fixity, and hence full shear or moment capacity will never be mobilized even at 4% lateral drift. But it is very difficult to fix the percentage of moment capacity for which the column base can be designed as several parameters need to be investigated. Hence, to be on the safe side, the design is done for M_{pc} or H_{pc}. The above observations show that base plate and anchor bolt flexibility can prevent formation of plastic hinge in the column, except in heavily loaded columns.

This study investigated the response of the most commonly used column base connection, namely, the anchor-bolted base plate connection, and improves the same by reinforcing the column-to-foundation joint. But, it is strongly felt that the associated base plate and anchor bolt flexibilities inhibit the formation of plastic hinge in the column itself, except in the heavily loaded columns, and as such, is not favorable to the desired sway mechanism. Thus, the use of other lateral load resisting systems, like shear walls, would be necessary in the direction of shaking corresponding to the weak-axis connections to reduce the drift demands on them.

8 Conclusions

The following salient conclusions are drawn from the study on weak-axis column-to-foundation connections in steel MRFs:

1. The combined action of *P*, *V* and *M* on column results in unsymmetrical stress distribution, particularly near the column-to-foundation joint with compression side of the column flange yielding prior to the tension side of the flange and webs.

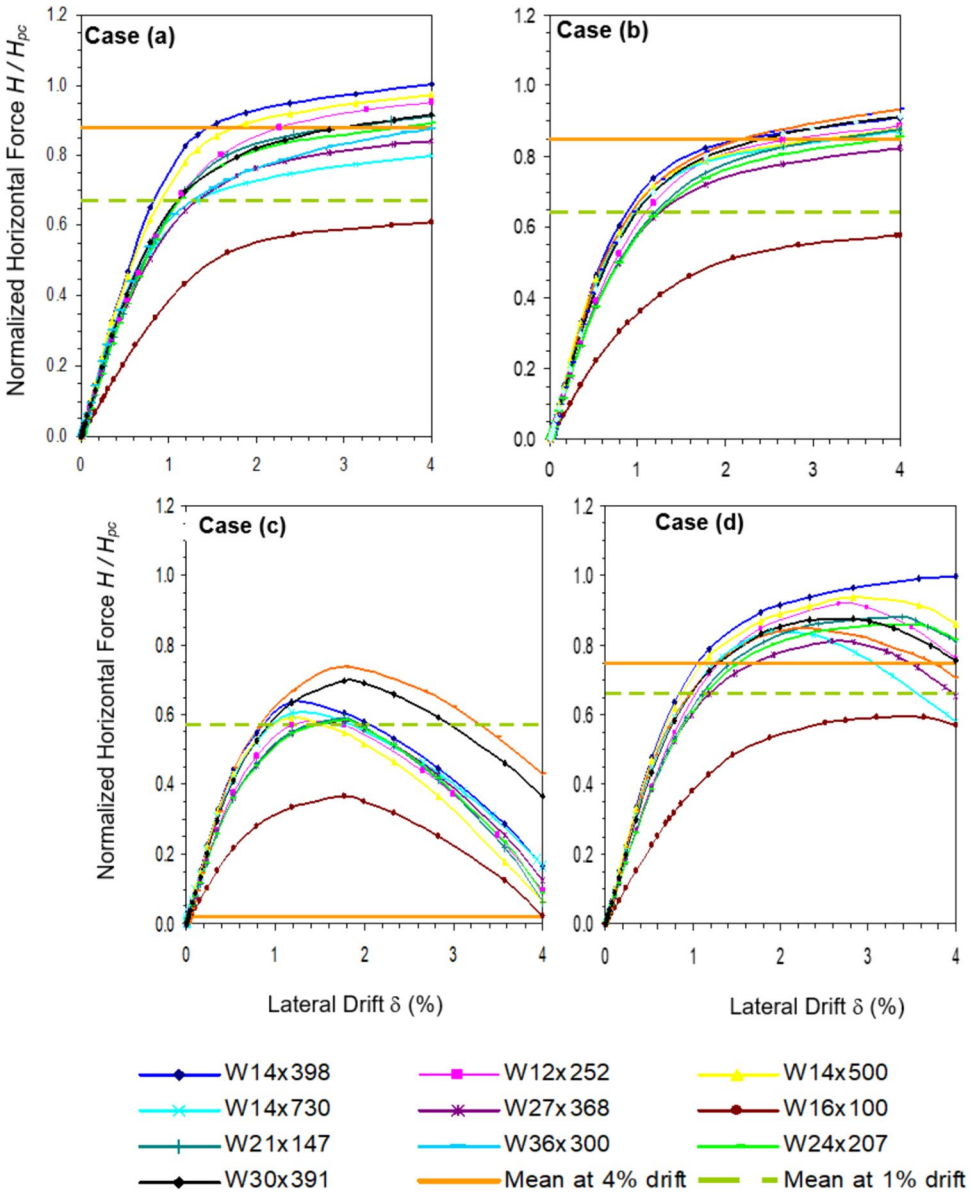

Fig. 10 *Inelastic response of 10 weak-axis column-to-foundation connection sub-assemblages for the four loading cases*: Maximum inelasticity is mobilized in interior heavily loaded columns (Case (b)). The dropping part in case (c) sub-assemblages is because of the axial force in the column reaching its yield capacity

2. Under pure shear loading, the truss length to depth ratio decreases from 0.41 at 0.33% drift to 0.36 at 1.00% drift, indicating a shift in inelastic behavior. With axial compressive load and bending moment, the truss length is lower, validating that the 0.5dc assumption is an upper bound, especially at higher drifts where anchor bolts yield and lose stiffness.
3. The observed truss length to column depth ratio is lower than assumed, and the efficiency of the configuration depends on the strength and stiffness of anchor bolts at higher drifts. Inelastic finite element analyses show that nonlinear response begins at about 0.55Hpc for load cases (a), (b), and (d), and at about 0.30Hpc for load case (c). Early nonlinear response is caused by tension yielding of anchor bolts and base plate uplift.
4. The AISC prescribed bilinear *P-M* interaction curve underestimates the column over strength capacity, and thus would result in conservative estimate of demands on the column-to-foundation connection.
5. At least in heavily loaded box-columns, the proposed cover-plated rib-platted connection configuration effectively reinforces the column at the column-to-foundation joint and forces the inelasticity to occur in the column away from the connection elements and welds.
6. Anchor-bolted base plate column-to-foundation connections are not suitable for use in weak-axis connections under seismic actions, without an alternative lateral load

Table 3 *Level of inelasticity mobilized in WACB joint-sub-assemblages at 1.00% drift*: Only about 50%-60% of column nominal plastic moment capacity is mobilized

Column Section	(H/H_{pc}) 1% Drift			
	Case (a) (0.2Py) + Pushover of (4%)	Case (b) (0.5Py) + Pushover of (4%)	Case (c) (0.5Py) + Pushover of (0.5Py and 4%)	Case (d) (0.5Py) + Pushover of (-0.4Py and 4%)
14×730	0.64	0.70	0.61	0.73
14×500	0.78	0.72	0.6	0.77
14×398	0.82	0.74	0.64	0.79
30×391	0.70	0.70	0.64	0.73
27×368	0.65	0.63	0.55	0.60
36×300	0.63	0.64	0.67	0.65
12×252	0.69	0.67	0.57	0.72
24×207	0.68	0.63	0.54	0.61
21×147	0.70	0.64	0.55	0.66
16×100	0.43	0.37	0.34	0.38
Average	**0.67**	**0.64**	**0.57**	**0.66**

Table 4 *Level of inelasticity mobilized in WACB joint-sub-assemblages at 4.00% drift*: Column nominal plastic moment capacity is not reached due to flexibilities of base plate and anchor bolts

Column Section	(H/H_{pc}) 4% Drift			
	Case (a) (0.2Py) + Pushover of (4%)	Case (b) (0.5Py) + Pushover of (4%)	Case (c) (0.5Py) + Pushover of (0.5Py and 4%)	Case (d)(0.5Py) + Pushover of (-0.4Py and 4%)
14×730	0.80	0.87	0.17	0.58
14×500	0.97	0.88	0.07	0.86
14×398	1.00	0.91	0.17	1.00
30×391	0.92	0.91	0.37	0.76
27×368	0.84	0.83	0.12	0.65
36×300	0.88	0.93	0.43	0.71
12×252	0.95	0.89	0.10	0.76
24×207	0.89	0.86	0.09	0.82
21×147	0.91	0.88	0.06	0.81
16×100	0.61	0.58	0.02	0.57
Average	**0.88**	**0.85**	**0.02**	**0.75**

resisting system, like a shear wall, to reduce the lateral drift demand.

7. The current connection configuration does not provide full fixity, preventing the mobilization of full shear or moment capacity (Mpc or Hpc) even at 4% lateral drift. Base plate and anchor bolt flexibility hinder plastic hinge formation in the column, necessitating the use of Mpc or Hpc for safe design. To achieve the desired sway mechanism, alternative lateral load resisting systems like shear walls are recommended to reduce drift demands on weak-axis connections.

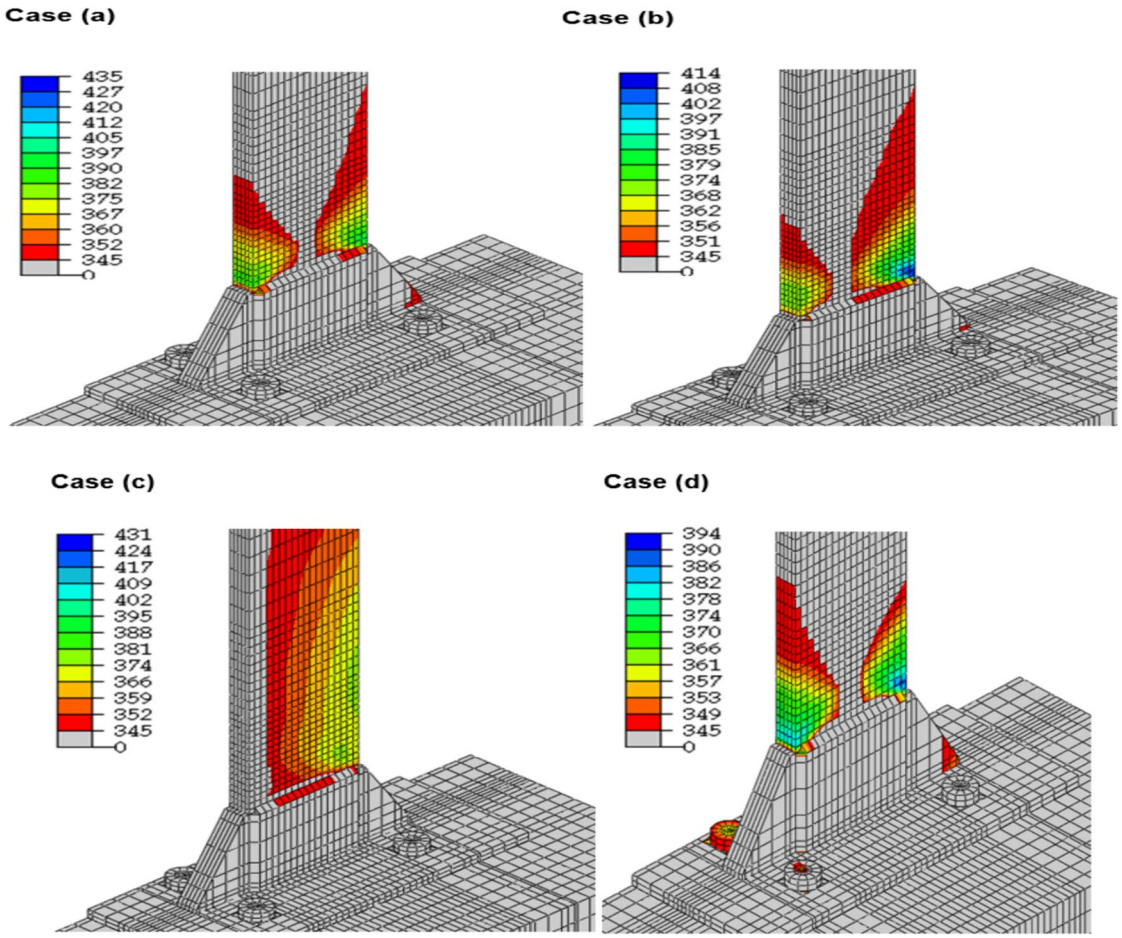

Fig. 11 *Typical yielding zones (von Mises stress Mpa exceeding the yield strength of the material in W14×398) weak-axis column-to-foundation connection sub-assemblages at 4% lateral drift for the four loading cases*: Only in the heavily loaded cases, inelasticity is developed in the columns. Also, the CJP welds connecting the column to the base plate are not stressed beyond the design strength

Funding The authors declare that no funds were received during the preparation of this manuscript.

Declarations

Conflict of interest The authors have no relevant financial or non-financial interests to disclose.

References

ACI 318–02 / ACI 318R-02, (2002). Building code requirements for structural concrete and commentary. American Concrete Institute, Farmington Hills, USA, 2002

Aviram, A. and Stojadinovic, B. (2006). Evaluation of design methods for column-base plate connections in gravity and moment resisting frames. *Proceedings of the 8th U.S. national conference on earthquake engineering,* San Francisco, California, Paper No 1269

Bertero, V.V., Anderson, J.C., and Krawinkler, H., (1994). Performance of steel building structures during the Northridge Earthquake. Report No. UCB/EERC-94/09, Earthquake Engineering Research Center, College of Engineering, University of California at Berkeley

Cannon, R. W. (1992). Flexible baseplates: effect of plate flexibility and preload on anchor loading and capacity. *ACI Structural Journal, 89*(3), 315–324.

Cook R.A., Doerr, G.T., and Klingner, R.E., (1989). Design Guide for Steel-to-Concrete Connections. Research Report No. 1126–4F, Center for Transportation Research, The University of Texas at Austin, Austin, Texas.

Cook, R. A., & Klingner, R. E. (1992). Ductile multiple-anchor steel-to-concrete connections. *Journal of Structural Engineering, ASCE, 118*(6), 1645–1665.

Cui, Y., Wang, F., Yang, C., Li, H., & He, Y. (2021). Using composite yield mechanism to mitigate seismic damage to exposed steel column base connections. *Engineering Structures, 232*, 111877. https://doi.org/10.1016/j.engstruct.2021.111877

DeWolf, J. T. (1978). Axially loaded column base plates. *Journal of the Structural Division, ASCE, 104*(ST5), 781–794.

DeWolf, J. T., & Sarisley, E. F. (1980). Column base plates with axial loads and moments. *Journal of the Structural Division, ASCE, 106*(ST11), 2167–2184.

Drake, R. M., & Elkin, S. J. (1999). Beam-column base plate design - LRFD method. *Engineering Journal, AISC, 36*(1), 29–38.

FEMA-355E (2000). State of the Art Report on Past Performance of Steel Moment-Frame Buildings in Earthquakes. SAC Joint Venture, CA, USA

Goswami, R., (2008). Seismic design of welded connections in steel moment resisting frame buildings with square box columns. Doctor of Philosophy Thesis, Indian Institute of Technology Kanpur, India

Grilli, D., Jones, R., & Kanvinde, A. (2017). Seismic performance of embedded column base connections subjected to axial and lateral loads. *Journal of Structural Engineering, 143*(5), 04017010. https://doi.org/10.1061/(asce)st.1943-541x.0001741

Hawkins, N. M., Mitchell, D., & Roeder, C. W. (1980). Moment resisting connections for mixed construction. *Engineering Journal, 17*, 1–10.

HKS. (2005). *ABAQUS/Standard user's manual, Hibbitt, Karlsson & Sorensen*. RI, USA: ABAQUS Inc.

Krawinkler, H., Anderson, J., and Bertero, V. (1996). Steel buildings, earthquake spectra, earthquake engineering research institute. Supplement C to Volume 11, January 1996 – Northridge Earthquake of January 17, 1994 Reconnaissance Report, Volume2, pp. 25–47

Latour, M., Piluso, V., & Rizzano, G. (2014). Rotational behaviour of column base plate connections: Experimental analysis and modelling. *Engineering Structures, 68*, 14–23. https://doi.org/10.1016/j.engstruct.2014.02.037

Lynch, T. J., & Burdette, E. G. (1991). Some design considerations for anchors in concrete. *Structural Journal, 88*(1), 91–97.

Marsh, M. L., & Brudette, E. G. (1985). Anchorage of steel building components to concrete. *Engineering Journal, 22*, 33–39.

Peier, W. H. (1983). Model for pull-out strength of anchors in concrete. *Journal of Structural Engineering, ASCE, 109*(5), 1155–1173.

Rabbat, B. G., & Russell, H. G. (1985). Friction coefficient of steel on concrete or grout. *Journal of Structural Engineering, ASCE, 111*(3), 505–515.

Salmon, C. G., Schenker, L., & Johnston, B. G. (1957). Moment - rotation characteristics of column anchorages. *Transaction of ASCE, 122*(2852), 132–154.

Shipp, J. G., & Haninger, E. R. (1983). Design of headed anchor bolts. *Engineering Journal, 20*, 58–69.

Thambiratnam, D. P., & Paramasivam, P. (1986). Base plates under axial loads and moments. *Journal of Structural Engineering, ASCE, 112*(5), 1166–1181.

Ueda, T., Kitipornchai, S., & Ling, K. (1990). Experimental investigation of anchor bolts under shear. *Journalof Structural Engineering, ASCE, 116*(4), 910–924.

You, Y. C., & Lee, D. (2020). Effect of anchors on the seismic performance of exposed column-base plate weak-axis connections. *Journal of Building Engineering, 32*, 101803. https://doi.org/10.1016/j.jobe.2020.101803

Zhao, D., Shan, Y., Wang, P., & Xu, J. (2022). Seismic performance analysis of exposed column-base connections along minor axis. *Journal of Constructional Steel Research, 197*, 107430. https://doi.org/10.1016/j.jcsr.2022.107430

Publisher's Note Springer Nature remains neutral with regard to jurisdictional claims in published maps and institutional affiliations.

Springer Nature or its licensor (e.g. a society or other partner) holds exclusive rights to this article under a publishing agreement with the author(s) or other rightsholder(s); author self-archiving of the accepted manuscript version of this article is solely governed by the terms of such publishing agreement and applicable law.